전기분무 콘제트-드리핑 모드 변환

박건중† · 김호영* · 송성진*

Mode Change from Cone-jet to Dripping in Electrospraying

Kun Joong Park, Ho-Young Kim and Seung Jin Song

Key Words : Electrospraying(전기분무), Cone-jet(콘제트), Stability(안정성), Electrohydrodynamics(전기수력학)

Abstract

The mode change from Taylor cone-jet to dripping in electrospraying has been analytically investigated. The change has been predicted by the dynamic behavior of a liquid drop at the tip of the cone-jet. Conservation laws are applied to determine the upward motion of the drop, and an instability model of electrified jets is used to determine the jet breakup. Finally, for the first time, the analysis enables prediction of the transition in terms of the Weber number and electric Bond number. The predictions are in good agreement with experimental data.

기호설명

D : jet diameter (m)
E : electric field intensity (V/m)
F_e : electric force acting on the drop (kg m/s^2)
g_e : electric acceleration (m/s^2)
K : electrical conductivity (S/m)
k : wave number
l_n : necking distance (m)
M : drop mass (kg)
Q : flow rate (m^3/s)
q : charge (C)
R_0 : jet radius (m)
r_c : radius of the capillary needle (m)
S : cross section area of the jet (m^2)
t : time (s)
V_0 : jet velocity (m/s)
v : drop velocity (m/s)
z_0 : distance between needle and plate (m)

그리스문자

α : Taylor cone half-angle
γ : surface tension coefficient (kg/s^2)
ε : dielectric constant
ε_0 : electrical permittivity of vacuum
η : nondimensional flow rate
ρ : density (kg/m^3)
σ_s : surface charge density (C/m^2)
τ_n : necking time (s)
Φ_0 : applied voltage (V)
ω : frequency or growth rate (1/s)

하첨자

c : critical
e : electric
min: minimum
n : normal direction or necking
s : surface tension
z : axial direction

† 회원, 서울대학교 기계항공공학부
E-mail : kjpark2@snu.ac.kr
TEL : (02)880-1701 FAX : (02)883-0179
* 회원, 서울대학교 기계항공공학부

1. 서 론

Electrospraying refers to electrostatic or electrohydrodynamic spraying of liquids. When a liquid is pumped through a capillary needle under an electric potential on the order of several kV to several tens of kV, the liquid meniscus forms a unique cone shape at the needle tip. Also, a thin jet emits from the cone apex and a spray forms. Taylor (1964) first analyzed the existence of the cone shape and validated his theory with experiments.[1] Thus, the liquid cone is referred to as the Taylor cone.

However, much is still unknown about the Taylor cone-jet. It is not only because the analysis of electrohydrodynamic flow is complicated due to numerous parameters but also because the measurement of key variables is difficult. One major unresolved issue is the stability of the Taylor cone-jet. Specifically, it is important to predict the transition from the cone-jet mode to another mode such as the dripping mode. Fernandez de la Mora & Loscertales (1994) investigated the transition,[2] and since then it has been known that the mode change from cone-jet to dripping occurs when the nondimensional flow rate $\eta \equiv \sqrt{\rho K Q/\gamma\varepsilon\varepsilon_0}$, where ρ, K, γ, and ε are the density, electrical conductivity, surface tension coefficient, and dielectric constant of the liquid, ε_0 the permittivity in vacuum, and Q the flow rate, has a value of approximately 1. However, the critical value over which the Taylor cone-jet ensues has been different depending on various parameters and many researchers have tried to accurately predict the transition.[3-6] Nonetheless, the predictions have been difficult probably because the effects of the applied voltage and electrode geometry have not been considered.

Therefore, the objective of this paper is to predict the stability of the Taylor cone-jet, or the transition from the cone-jet mode to the dripping mode, through an analytical investigation. A new stability model of the Taylor cone-jet is presented and the transition has been predicted by the dynamics of a liquid drop at the tip of the cone-jet. Conservation laws and a jet instability model are applied to determine the upward drop motion and the jet breakup, respectively. The new model's predictions have been compared with experimental results.

2. 본 론

Consider a Taylor cone-jet before the transition to dripping as shown in figure 1(a). The Taylor cone retains its shape and a drop is attached to a thin thread emerging from the cone. The liquid is assumed to be inviscid. In figure 1(b), D is the diameter of the jet. Here D is assumed to be constant along the axial direction because the jet is slender. V_0 is the downward velocity of the jet, and the velocity profile across the jet is assumed to be uniform due to negligible viscous effects and small D.

2.1 Motion of the drop moving towards the cone

In figure 1(b), ζ is the displacement of the drop and t the time. If at $t = 0$ a drop completely detaches from the jet, the remaining part of the jet begins to recede upward towards the cone and a new drop is formed at $\zeta = 0$. The mass of the drop, M, gradually increases during the recession:

$$M = \rho S(\zeta + V_0 t), \tag{2.1}$$

where S is the cross-section area of the jet and $S \equiv \pi D^2/4$. If v is the velocity of the drop, the equation of motion of the drop can be written in the form

$$\frac{d}{dt}(Mv) = \pi D\gamma - \rho S V_0 (v + V_0) - F_e, \tag{2.2}$$

where F_e represents the electric force downward. Here the surface tension force is calculated with D, not with the needle diameter as in Clanet & Lasheras (1999).[7] Substituting (2.1) into (2.2) and using $v = d\zeta/dt$, the equation of motion becomes

$$\frac{d}{dt}\left[(\zeta + V_0 t)\frac{d\zeta}{dt}\right] = V_s^2 - V_0\left(\frac{d\zeta}{dt} + V_0\right) - \frac{1}{\rho S}F_e, \tag{2.3}$$

where $V_s \equiv \sqrt{4\gamma/\rho D}$.

To solve (2.3), D needs to be determined. Thus, the so-called asymptotic universal scaling of D is adopted. The scaling, presented by Ganan-Calvo (1997), is

$$D = 2\pi^{-2/3}\left(\frac{\rho\varepsilon_0}{\gamma K}\right)^{1/6} Q^{1/2} f_b, \tag{2.4}$$

where f_b is a scaling constant.[8]

Then, F_e is the only undetermined part in (2.3), and is newly predicted. If q is the net charge of the drop and E_0 the axial electric field acting on the drop,

$$F_e = qE_0, \tag{2.5}$$

by Coulomb's law. Charges are assumed to relax and accumulate to the liquid surface immediately, and therefore the liquid inside is regarded as quasi-neutral. And q is assumed to be as the sum of two parts, one from the remaining part of the jet after the breakup and the other from the upstream jet. Thus (2.5) becomes

$$F_e = \pi D(\zeta + V_0 t)\sigma_s E_0, \qquad (2.6)$$

where σ_s is the surface charge density of the jet.

To determine σ_s, the normal electric boundary condition at the liquid-gas interface is invoked as

$$\sigma_s = \varepsilon_0 E_n - \varepsilon\varepsilon_0 E_n^{\,i} \approx \varepsilon_0 E_n, \qquad (2.7)$$

where E_n and $E_n^{\,i}$ represent the outer and inner electric fields normal to the surface respectively. And the normal stress balance at the jet surface gives

$$\frac{2\gamma}{D} = \frac{1}{2}\varepsilon_0 E_n^{\,2}. \qquad (2.8)$$

Hence, from (2.4), (2.7) and (2.8), σ_s is newly determined as

$$\sigma_s = \left(\frac{4\gamma\varepsilon_0}{D}\right)^{1/2} = \pi^{1/3}(2\gamma\varepsilon_0)^{1/2}\left(\frac{\gamma K}{\rho\varepsilon_0}\right)^{1/12} Q^{-1/4} f_b^{\,-1/2}. \qquad (2.9)$$

In (2.6), E_0 also needs to be determined, and is newly approximated as the axial component of the maximum normal electric field of the cone, $E_{n,\max}$, due to the small size of the drop (figure 2). Then we get

$$E_0 \approx E_{n,\max}\sin\alpha = \left(\frac{4\gamma\cos\alpha}{\varepsilon_0 D}\right)^{1/2}\sin\alpha, \qquad (2.10)$$

where α is the Taylor cone half-angle.

α is known to depend on variables such as the applied voltage and the flow rate (Ganan-Calvo, Pantano & Barrero 1996).[9] Therefore, a correlation for α is presented by scaling the axial electric field at the needle tip, E_z. Jones & Thong (1971) calculated E_z in needle-to-plate geometry by applying the image method:

$$E_{z,image} \approx \frac{\Phi_0}{r_c \ln(4z_0/r_c)}, \qquad (2.11)$$

where Φ_0 and r_c are the applied voltage and radius of the needle, respectively.[10] Also, E_z is determined from the normal stress balance as

$$E_{z,Taylor} = \left(\frac{2\gamma\cos\alpha}{\varepsilon_0 r_c}\right)^{1/2}\sin\alpha. \qquad (2.12)$$

From (2.11) and (2.12),

$$\sqrt{\cos\alpha}\sin\alpha = \frac{C_a}{\sqrt{2}}\left(\frac{\varepsilon_0}{\gamma}\right)^{1/2}\frac{\Phi_0}{r_c^{1/2}\ln(4z_0/r_c)}, \qquad (2.13)$$

where C_a is a scaling constant. Here a key nondimensional parameter in electrospraying, the electric Bond number Bo_E, is derived as

$$Bo_E \equiv \left(\frac{\varepsilon_0}{\gamma}\right)^{1/2}\frac{\Phi_0}{r_c^{1/2}\ln(4z_0/r_c)}. \qquad (2.14)$$

Bo_E represents the ratio of electric force to surface tension. Figure 3 shows the correlation between $\sqrt{\cos\alpha}\sin\alpha$ and Bo_E according to the data obtained experimentally by Ganan-Calvo et al. (1996) and C_a has a value of 1.583.

The substitution of (2.6) into (2.3) yields an analytic solution for ζ:

$$\zeta = -\frac{g_e}{6}t^2 + (V_s - V_0)t, \qquad (2.15)$$

where "acceleration of electric force" $g_e \equiv 4\sigma_s E_0/\rho D$, termed analogous to that of gravity. From (2.15), the maximum displacement of the drop,

$$\zeta_{\max} = \frac{3(V_s - V_0)^2}{2g_e}. \qquad (2.16)$$

2.2 Jet breakup or necking

Once the drop reaches $\zeta_{\max}$, the drop begins to move downward and detach from the jet. This jet breakup is called necking. Basset (1894) and Taylor (1969) analyzed the breakup of electrified jets and presented an dispersion relation as

$$\omega^2\left[\frac{\rho R I_0(kR)}{kI_1(kR)}\right] = \frac{\gamma}{R^2}(1-k^2R^2) - \frac{\varepsilon_0\Phi_0^{\,2}}{R^3[\ln(r_0/R)]^2}\left[1-\frac{kRK_1(kR)}{K_0(kR)}\right], \qquad (2.17)$$

where k, R, and r_0 are the wave number, the jet radius, and the distance between the jet and the earthed radial surrounding respectively, and I_0, I_1, K_0, and K_1 the modified Bessel functions.[11,12] From (2.17), the necking time τ_n can be written as

$$\tau_n = C_n\left(\frac{\rho D^3}{8\gamma}\right)^{1/2}, \qquad (2.18)$$

where C_n is a scaling factor known to be 2.91 for non-electrified jets. Here C_n is written in terms of Bo_E as

$$C_n = \frac{(Bo_E - C_0)^2}{Bo_E}, \qquad (2.19)$$

where C_0 is constant.

If the drop moves downward a distance l_n during the jet breakup, then

$$l_n \approx V_0 \tau_n , \qquad (2.20)$$

where l_n is called the necking distance.

2.3 Transition from cone-jet to dripping

If $l_n < \zeta_{\max}$, the necking point moves upward. Therefore, at this condition, the cone-jet mode transitions to the dripping mode. On the other hand, if $l_n > \zeta_{\max}$, the necking point moves downward so that the jet is extended and thus maintained. Consequently, the transition condition is $l_n = \zeta_{\max}$, and from (2.16) and (2.20), it becomes

$$\frac{V_0}{V_s} = 1 + \frac{g_e \tau_n}{3V_s} - \left[\left(1 + \frac{g_e \tau_n}{3V_s} \right)^2 - 1 \right]^{1/2} . \qquad (2.21)$$

Here V_0/V_s is replaced with the Weber number defined as $We \equiv \rho V_0^{\,2} D/\gamma$. We is the ratio of inertia to surface tension and $We = 4(V_0/V_s)^2$. Finally, from (2.9), (2.10), (2.13), (2.14), (2.18) and (2.21), the transition condition, in terms of We and Bo_E, is

$$Bo_E = \frac{3}{2} \frac{1}{C_n C_a} \left[\frac{1}{4} \sqrt{We} + \frac{1}{\sqrt{We}} - 1 \right] . \qquad (2.22)$$

Also, from (2.4), We can be replaced with η. Given Q, V_0 is written as

$$V_0 = \frac{4Q}{\pi D^2} = \pi^{-1/3} \left(\frac{\rho \varepsilon_0}{\gamma K} \right)^{-1/3} \frac{1}{f_b^{\,2}} , \qquad (2.23)$$

and therefore, the relationship between We and η is newly given by

$$We = \frac{2\sqrt{\varepsilon}}{f_b^{\,3}} \eta . \qquad (2.24)$$

Thus, the transition condition, in terms of η and Bo_E, is

$$Bo_E = \frac{3}{2} \frac{1}{C_n C_a} \left[\frac{1}{4} \frac{\sqrt{2}\varepsilon^{1/4}}{f_b^{\,3/2}} \sqrt{\eta} + \frac{f_b^{\,3/2}}{\sqrt{2}\varepsilon^{1/4}} \frac{1}{\sqrt{\eta}} - 1 \right] . \qquad (2.25)$$

2.4 Determination of f_b and C_0

Tang & Gomez (1994) provide all of the relevant information, which includes a stability diagram as shown in figure 4.[13] By matching the critical or discontinuous point which is found in both the model and the experiment, f_b and C_0 are determined.

η at the critical point is

$$\eta_c = \frac{2 f_b^{\,3}}{\sqrt{\varepsilon}} , \qquad (2.26)$$

and Bo_E at the critical point is

$$Bo_{E,c} = C_0 . \qquad (2.27)$$

In the experiments of Tang & Gomez (1994), $\eta_c = 0.688$ and $Bo_{E,c} = 1.25$. Hence from (2.26) and (2.27), $f_b = 1.46$ and $C_0 = 1.25$.

3. 결과 및 토의

Figure 5 shows a comparison of the predicted and measured transition conditions. The agreement is excellent. Here, if we divide the transition condition into two parts based on the critical point, with increasing η, Bo_E at the transition decreases in the left but increases in the right. This "V" shape forms because, in (2.25), the term involving $1/\sqrt{\eta}$ dominates the left and the term involving $\sqrt{\eta}$ the right.

Another set of experimental data is found in Cloupeau & Prunet-Foch (1989).[14] Figure 6 shows the measured transition condition along with the predictions. Here, to find causes of a discrepancy, the values of key experimental parameters are examined (Table 1). Among many experimental parameters, ε may be responsible for the discrepancy because it is not included in the scaling of D, (2.4). In Table 1, the value of ε is 4.29, which is very small compared to 80 of Tang & Gomez's (1994) experiments. Therefore, the scaling of D, (2.4), may be adequate for large values of ε, and may need to be further refined for small values of ε.

In figure 4, at a certain point in the cone-jet mode, if Q is decreased at a fixed Φ_0, the mode transition occurs. Q corresponding to this transition is called the minimum flow rate $Q_{\min}$, and is clearly dependent on Φ_0. In our analysis, $\sqrt{\cos\alpha}\sin\alpha$, which can be interpreted as the nondimensional axial electric field acting on the drop, depends on Φ_0 in (2.13), and the mode transition to dripping is predicted in terms of Φ_0 as shown in figure 5. Nevertheless, another prediction of the transition to the multi-jet mode, which corresponds to the upper boundary of the cone-jet mode in figure 4, is needed to determine the condition for $Q_{\min}$ completely.

4. 결 론

The transition from the Taylor cone-jet mode to the dripping mode has been analyzed, and, for the first time, the transition has been accurately predicted. Therefore, the mechanism behind this transition is concluded to be based on the dynamic behaviour of the drop at the tip of the cone-jet with the following remarks. The surface tension force, jet inertia, and electric force determine the transition, and these three forces are represented as two nondimensional parameters; the Weber number We and the electric Bond number Bo_E. The minimum value of η over which the cone-jet mode is maintained is determined in terms of Bo_E, defined as $Bo_E \equiv (\sqrt{\varepsilon_0/\gamma r_c}/\ln(4z_0/r_c))\Phi_0$. A function of the Taylor cone half-angle, $\sqrt{\cos\alpha}\sin\alpha$, is regarded as the nondimensional axial electric field acting on the drop, and is also determined from Bo_E.

후 기

The authors acknowledge the useful comments of Professor M. Martinez-Sanchez and Professor P. C. Lozano at MIT and Professor A. M. Ganan-Calvo at Universidad de Sevilla, Spain. The authors are grateful to the financial support from the Micro Thermal System Research Center sponsored by the Korea Science and Engineering Foundation.

참고문헌

(1) Taylor, G. I., 1964, "Disintegration of water drops in an electric field," *Proc. R. Soc. London, Ser. A*, Vol. 280, pp. 383-397.

(2) Fernandez de la Mora, J. and Loscertales, I. G., 1994, "The current emitted by highly conducting Taylor cones," *J. Fluid Mech.*, Vol.260, pp. 155-184.

(3) Ganan-Calvo, A. M., 1994, "The size and charge of droplets in the electrospraying of polar liquids in cone-jet mode, and the minimum droplet size," *J. Aerosol Sci.*, Vol. 25, pp. S309-S310.

(4) Chen, D.-R., Pui, D. Y. H. and Kaufman, S. L., 1995, "Electrospraying of conducting liquids for monodisperse aerosol generation in the 4 nm to 1.8 μm diameter range," *J. Aerosol Sci.*, Vol. 26, pp. 963-977.

(5) Chen, D.-R. and Pui, D. Y. H., 1997, "Experimental investigation of scaling laws for electrospraying: Dielectric constant effect," *Aerosol Sci. Technol.*, Vol. 27, pp. 367-380.

(6) Ganan-Calvo, A. M., Davila, J. and Barrero, A., 1997, "Current and droplet size in the electrospraying of liquids. Scaling laws," *J. Aerosol Sci.*, Vol. 28, pp. 249-275.

(7) Clanet, C. and Lasheras, J. C., 1999, "Transition from dripping to jetting," *J. Fluid Mech.*, Vol. 383, pp. 307-326.

(8) Ganan-Calvo, A. M., 1997, "Cone-jet analytical extension of Taylor's electrostatic solution and the asymptotic universal scaling laws in electrospraying," *Phys. Rev. Lett.*, Vol. 79, pp. 217-220.

(9) Ganan-Calvo, A. M., Pantano, C. and Barrero, A., 1996, "The equilibrium shapes of liquid menisci emitting liquid and charges in steady cone-jet mode," *J. Aerosol Sci.*, Vol. 27, pp. S187-S188.

(10) Jones, A. R. and Thong, K. C., 1971, "The production of charged monodisperse fuel droplets by electrical dispersion," *J. Phys. D: Appl. Phys.*, Vol. 4, pp. 1159-1166.

(11) Basset, A. B., 1894, "Waves and jets in a viscous liquid," *Am. J. Math.*, Vol. 16, pp. 93-110.

(12) Taylor, G. I., 1969, "Electrically driven jets," *Proc. R. Soc. London, Ser. A*, Vol. 313, pp. 453-475.

(13) Tang, K. and Gomez, A., 1994, "Generation by electrospray of monodisperse water droplets for targeted drug delivery by inhalation," *J. Aerosol Sci.*, Vol. 25, pp. 1237-1249.

(14) Cloupeau, M. and Prunet-foch, B., 1989, "Electrostatic spraying of liquids in cone-jet mode," *J. Electrostat.*, Vol. 22, pp. 135-159.

Table 1 Values of key experimental parameters along with η_c and $Bo_{E,c}$ of Tang & Gomez's (1994) and Cloupeau & Prunet-Foch's (1989) experiments

Parameters	Tang & Gomez (1994)	Cloupeau & Prunet-Foch (1989)

Flow rate (m^3/s)	~10^{-10}	10^{-11}~10^{-8}
Applied voltage (kV)	13.4~16.0	3.31~3.88
Surface tension coeff. (N/m)	7.30 x 10^{-2}	3.50 x 10^{-2}
Electrical conductivity (S/m)	1.02 x 10^{-4}	3.20 x 10^{-7}
Dielectric constant	80	4.29
Nondimensional flow rate η_c	0.688	0.772
Electric Bond number $Bo_{E,c}$	1.25	0.537

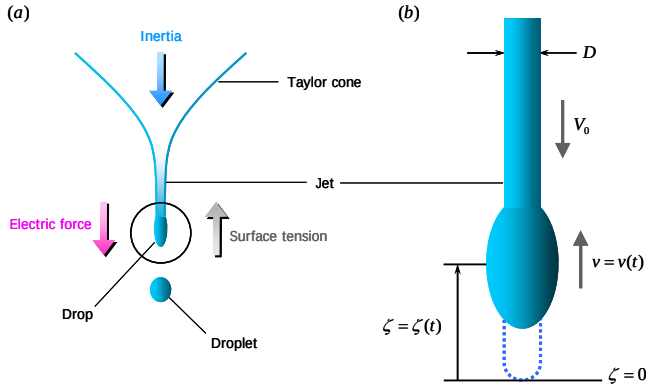

Fig. 1 A drop at the tip of the Taylor cone-jet. (a) Three external forces acting on the drop; (b) motion of the drop moving towards the cone.

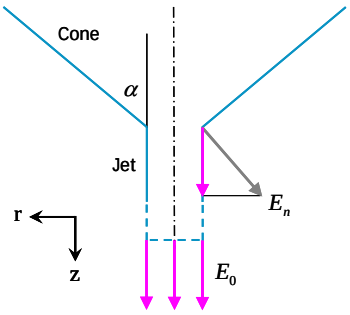

Fig. 2 Axial electric field acting on the drop.

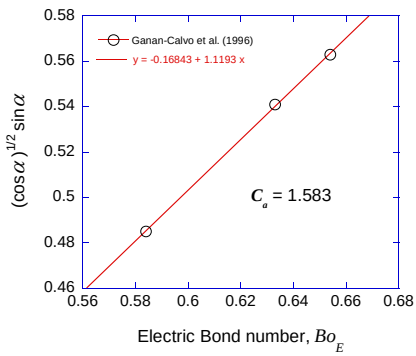

Fig. 3 Correlation between $\sqrt{\cos\alpha}\sin\alpha$ and Bo_E.

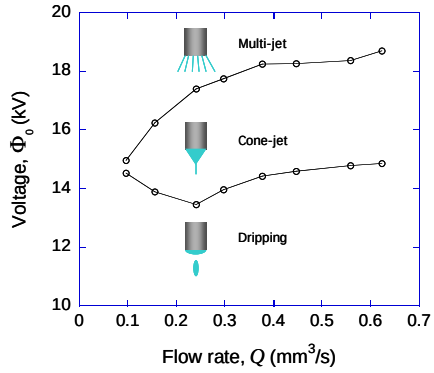

Fig. 4 Stability diagram provided by Tang & Gomez (1994).

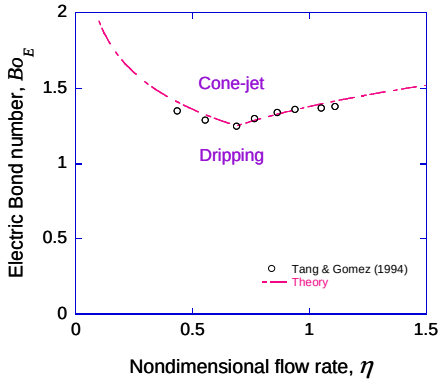

Fig. 5 Predicted and measured transition conditions in terms of η and Bo_E.

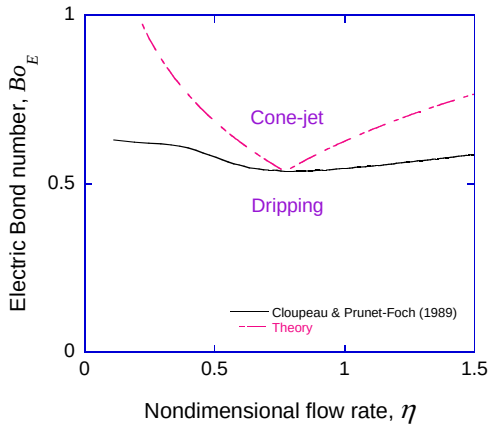

Fig. 6 Comparison of the predicted and measured transition conditions. The experimental data are from Cloupeau & Prunet-Foch (1989).